Electronic Supplementary Information

Alkylsilyl-Substituted Benzodithiophene-Based Small Molecules As Promising Hole-Transport Materials For Perovskite Solar Cells†

M. E. Sideltsev, A. N. Zhivchikova, I. E. Kuznetsov, D. K. Sagdullina, M. M. Tepliakova, A. A. Piryazev, D. V. Anokhin, M. S. Maksimovich, N. G. Nikitenko, D. A. Ivanov, and A. V. Akkuratov

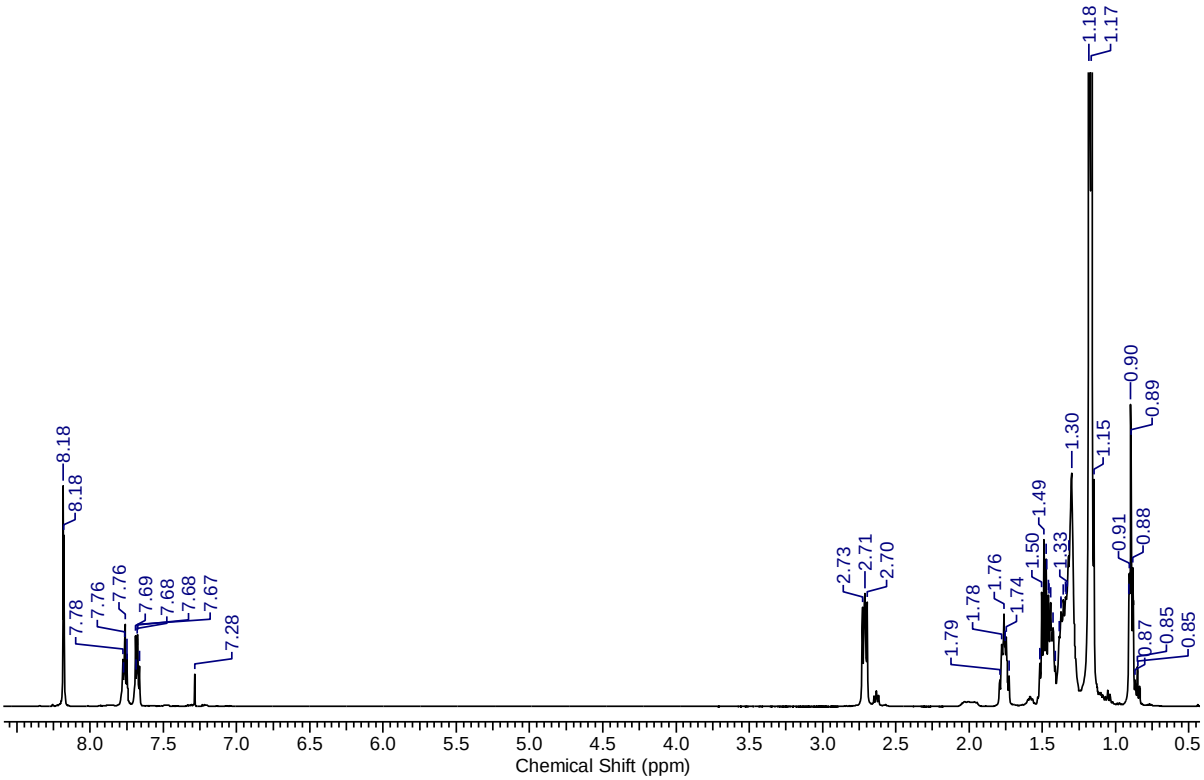

Figure S1. ^{1}H NMR spectrum of compound **2**.

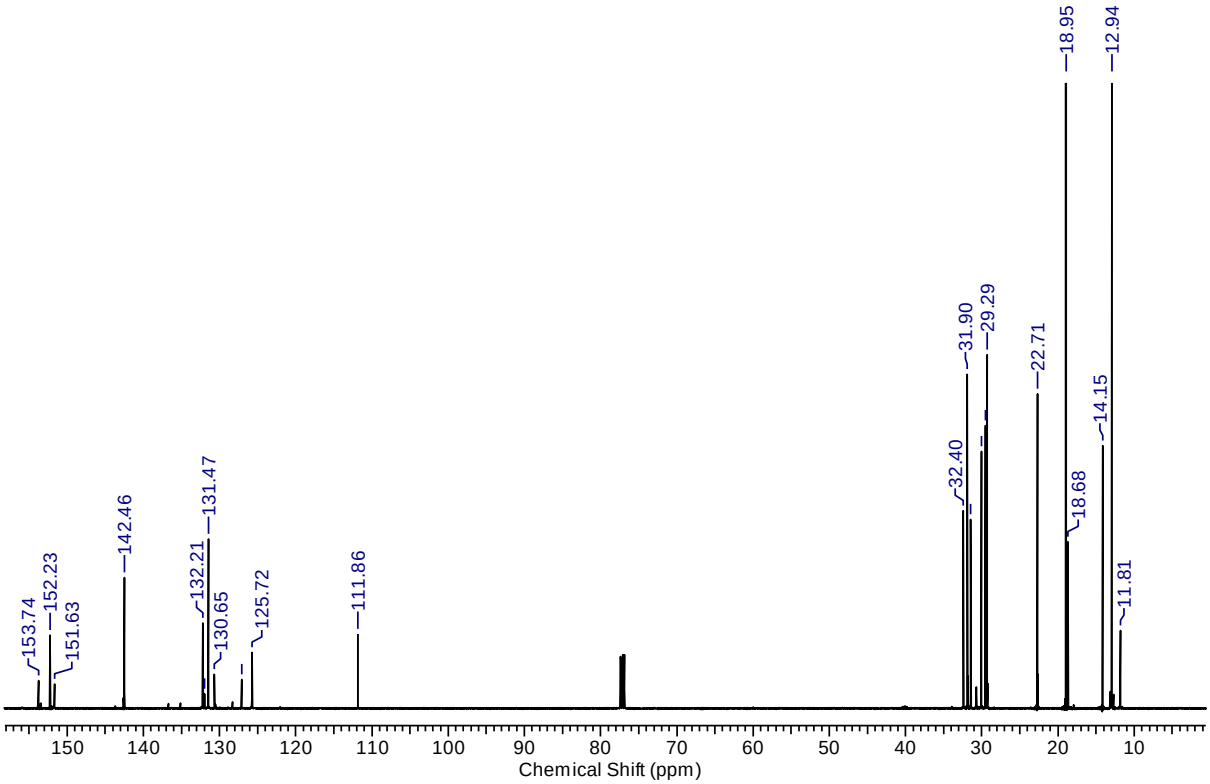

Figure S2. ^{13}C NMR spectrum of compound **2**.

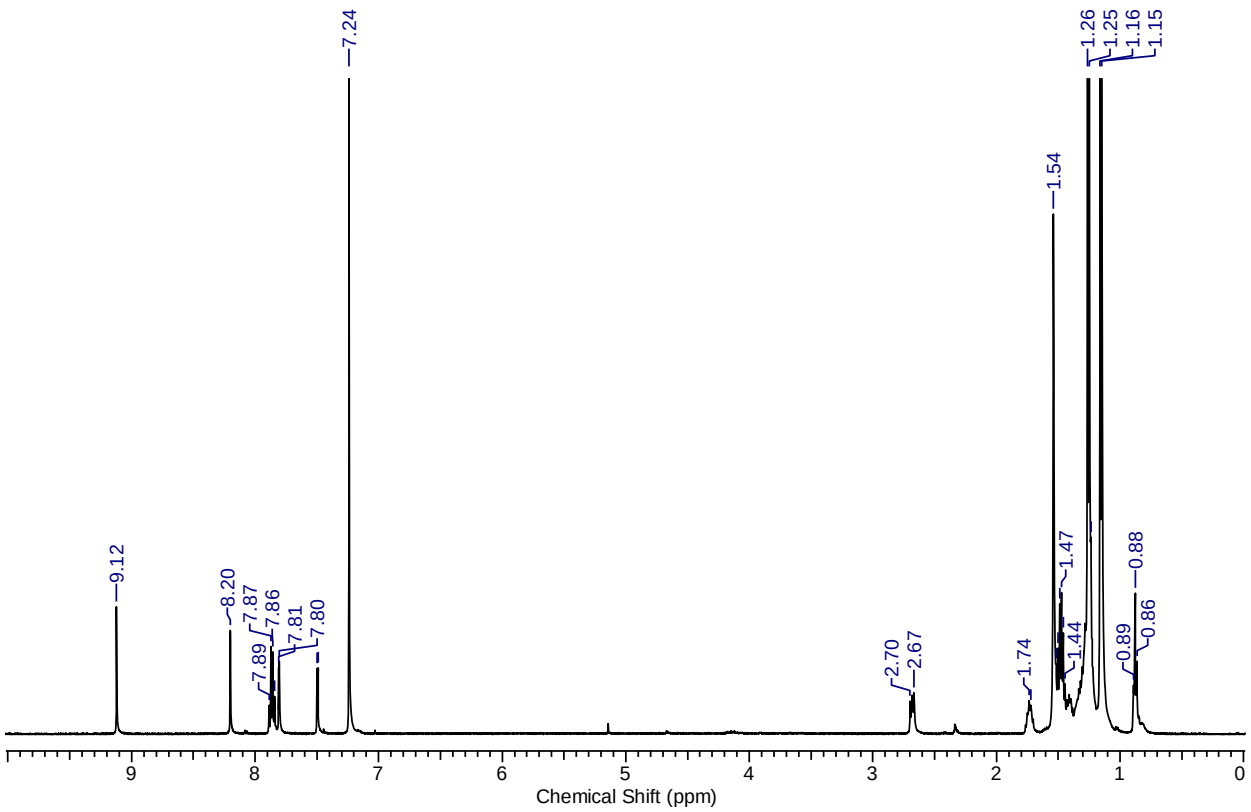

Figure S3. ^{1}H NMR spectrum of **TB-Si$_{3\text{-}3}$**.

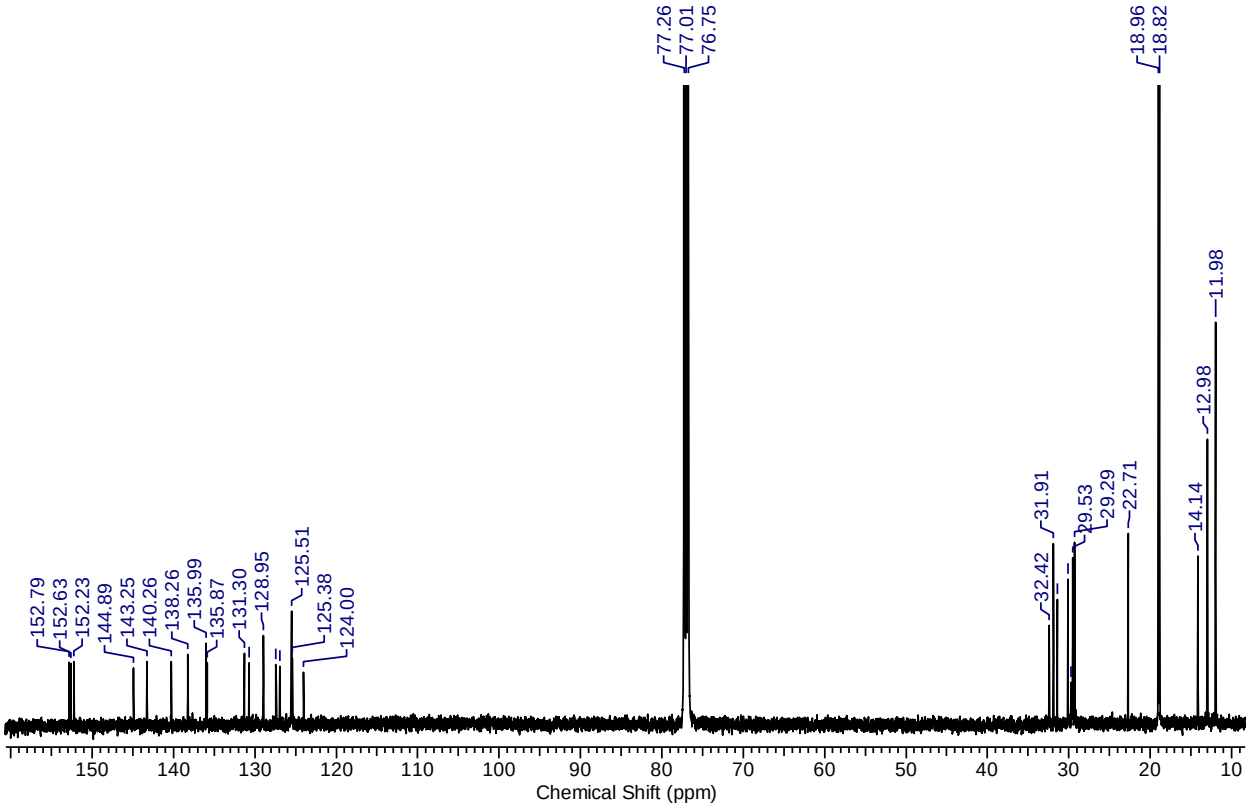

Figure S4. ^{13}C NMR spectrum of **TB-Si$_{3\text{-}3}$**.

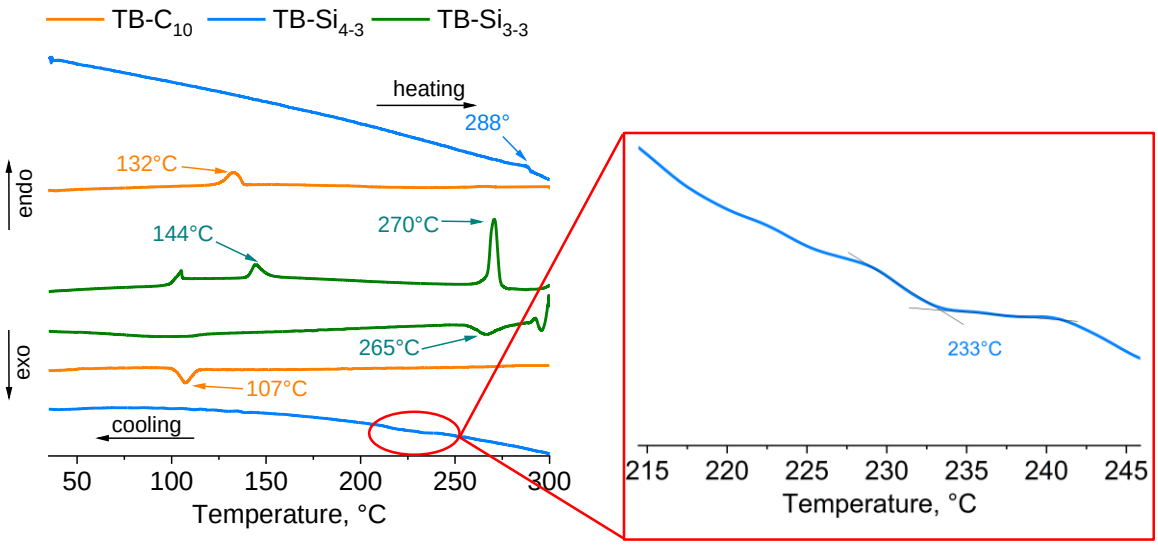

Figure S5. DSC plots for small molecules **TB-C$_{10}$**, **TB-Si$_{4-3}$**, and **TB-Si$_{3-3}$**

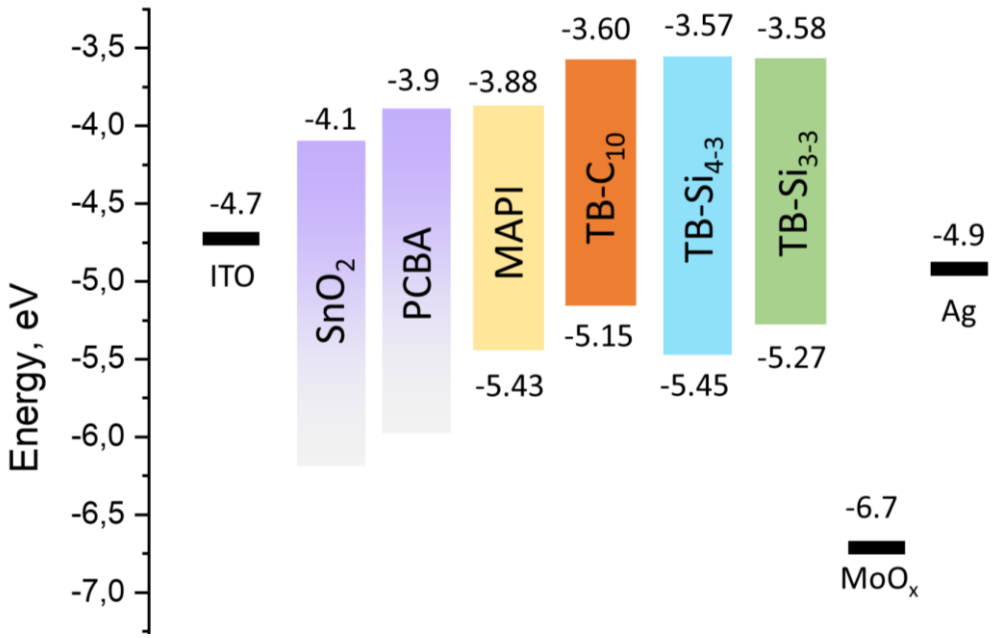

Figure S6. Energy level diagram of components of PSCs.

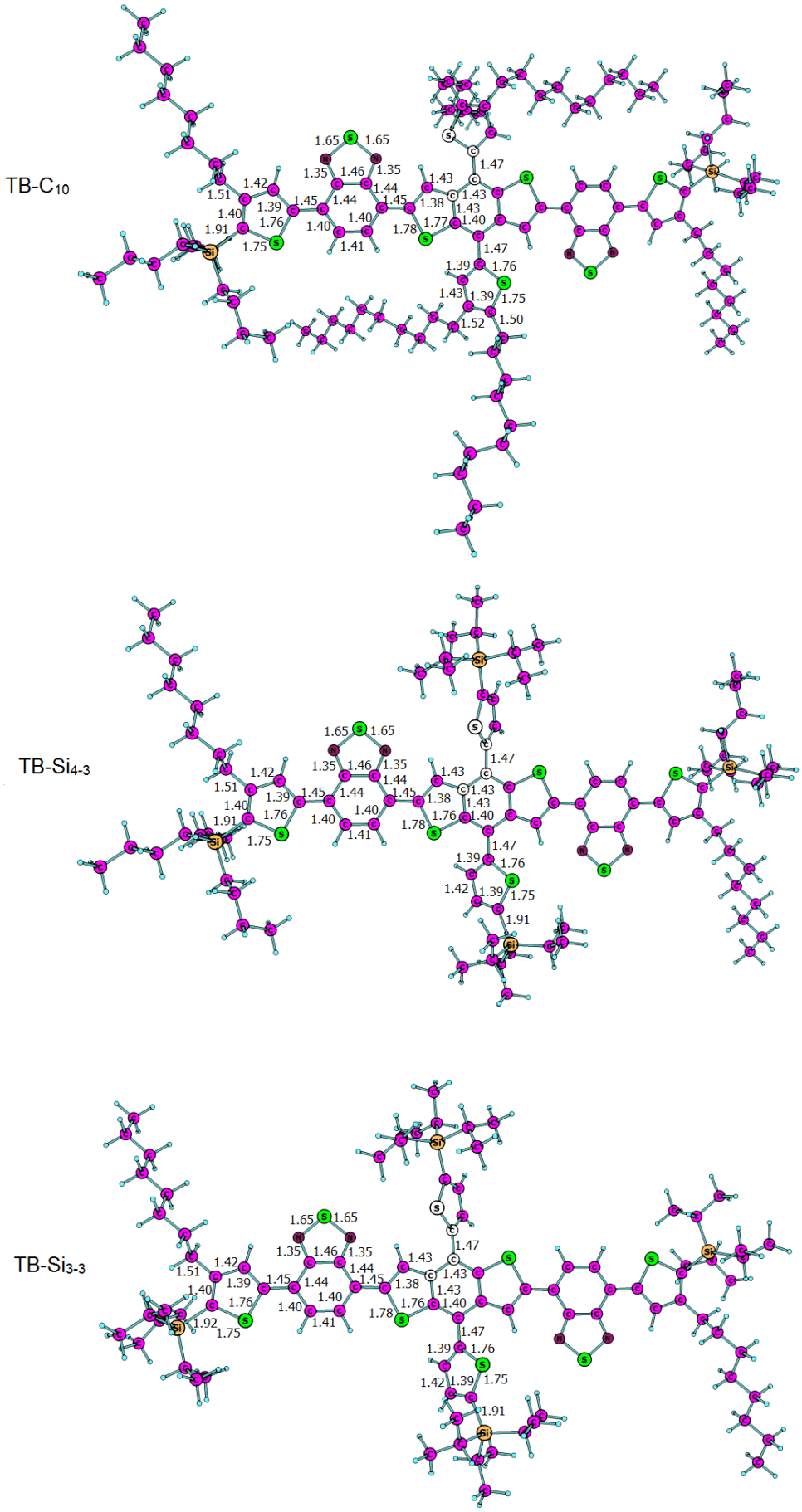

Figure S7. The optimized geometry of the **TB-C$_{10}$**, **TB-Si$_{4\text{-}3}$**, **TB-Si$_{3\text{-}3}$**. Distances between atoms are indicated in Å.

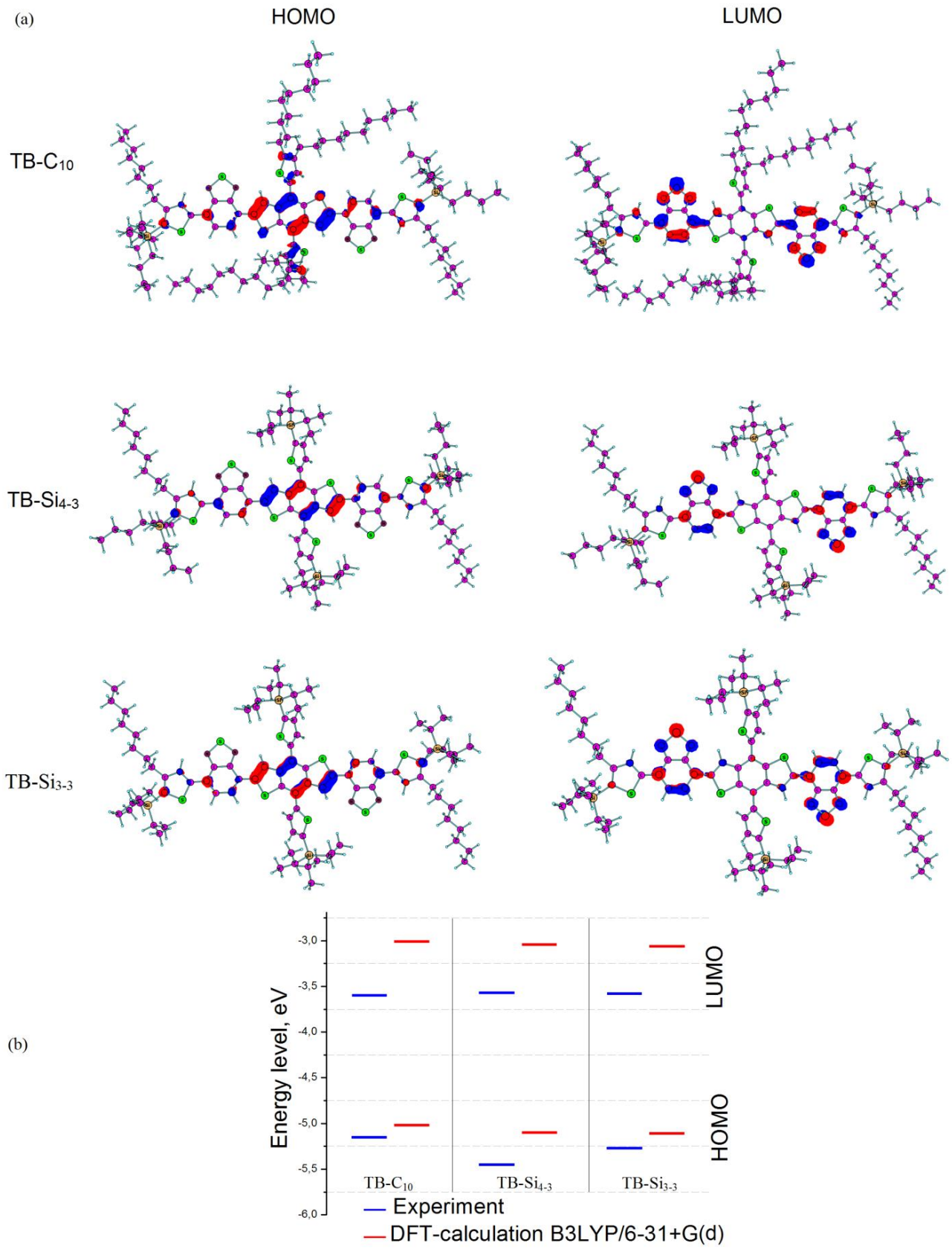

Figure S8. HOMO and LUMO distribution for **TB-C$_{10}$**, **TB-Si$_{4-3}$**, **TB-Si$_{3-3}$** (a); and frontier molecular orbital energy levels as estimated from experiment and predicted by B3LYP/6-31+G(d) calculations (b).

Table S1. HOMO/LUMO energies and energy gaps (E_g) for **TB-C$_{10}$**, **TB-Si$_{4-3}$**, **TB-Si$_{3-3}$** calculated using the PBE/6-31+G(d) and B3LYP/6-31+G(d) approaches in comparison with experimental data.

	HOMO/ LUMO, eV			**E_g, eV**			
	Calculation		**Experiment**	**Calculation**		**Experiment**	
	PBE/ 6-31+G(d)	**B3LYP/ 6-31+G(d)**		**PBE/ 6-31+G(d)**	**B3LYP/ 6-31+G(d)**	E_g^{CV}	E_g^{opt}
TB-C$_{10}$	-4.49/-3.41	-5.02/-3.01	-5.15/-3.60	1.08	2.01	1.55	1.99
TB-Si$_{4-3}$	-4.58/-3.45	-5.10/-3.04	-5.45/-3.57	1.13	2.06	1.88	2.05
TB-Si$_{3-3}$	-4.60/-3.46	-5.11/-3.06	-5.27/-3.58	1.14	2.05	1.69	2.05

HTM	V_{OC}, mV	J_{SC}, mA cm^{-2}	FF,%	PCE,%
Spiro-OMeTAD	910±60	16.1±0.5	46±10	7.0±2.0

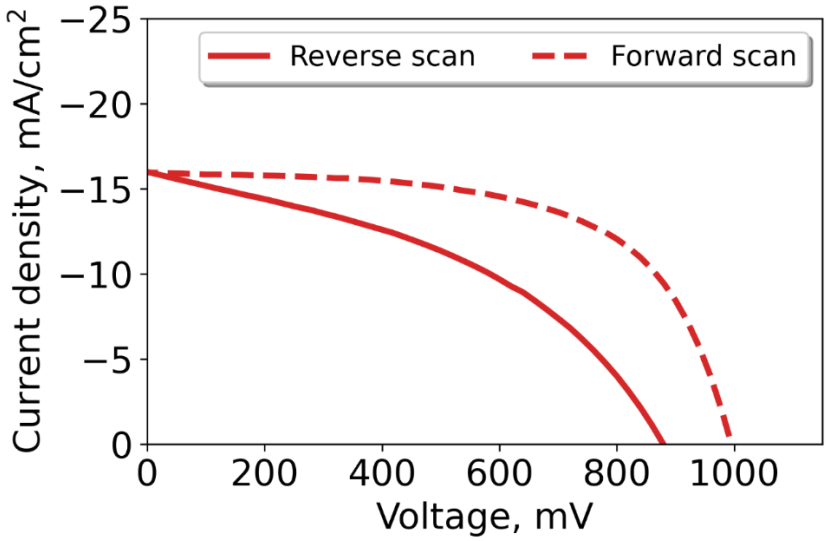

Figure S9. *J*-V curve for PSCs with non-doped spiro-OMeTAD as HTM.

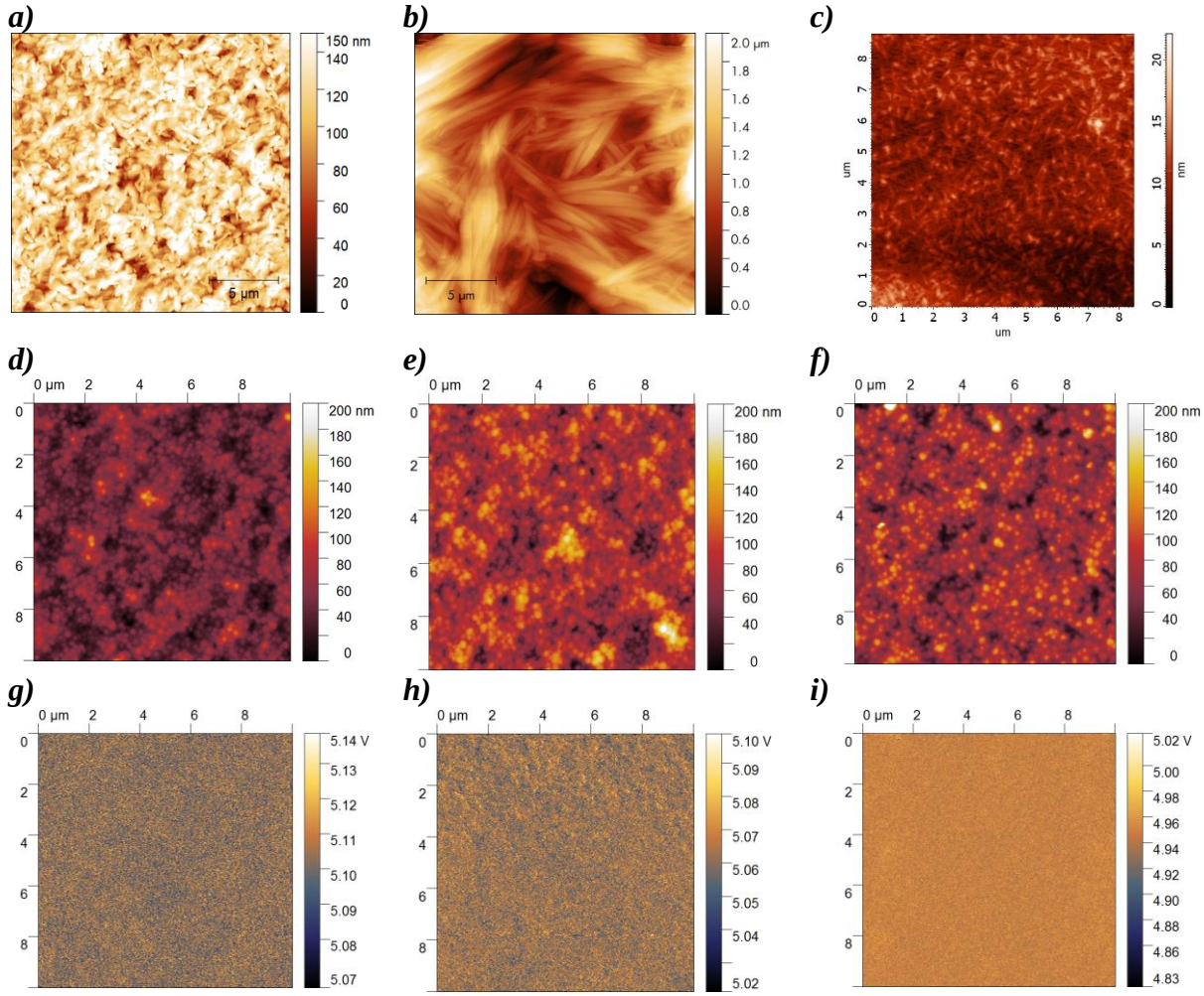

Figure S10. AFM images for thin films of **TB-C$_{10}$** (***a***), **TB-Si$_{4\text{-}3}$** (***b***) and **TB-Si$_{3\text{-}3}$** (***c***) deposited from chlorobenzene. AFM (***d, e, f***) and surface potential images (***g, h, i***) of $MAPbI_3$/**TB-C$_{10}$**, $MAPbI_3$/**TB-Si$_{4\text{-}3}$**, $MAPbI_3$/**TB-Si$_{3\text{-}3}$**, respectively.

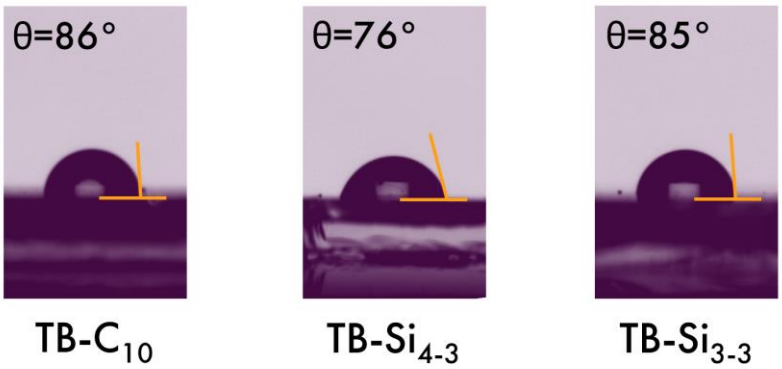

Figure S11. Contact angle of water on the surface of $MAPbI_3$/HTMs.

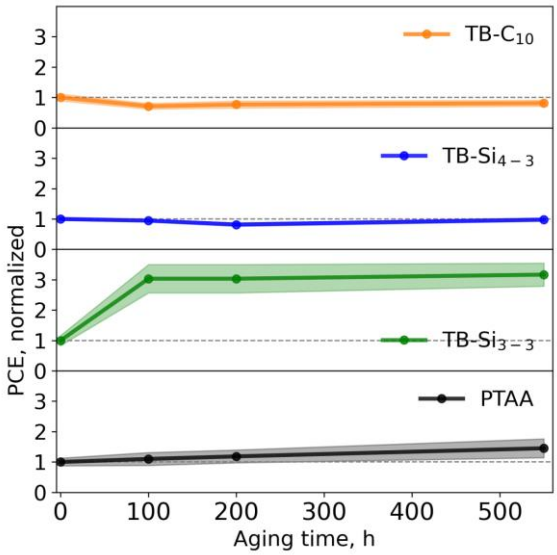

Figure S12. Evolution of relative power conversion efficiency of perovskite solar cells incorporating **TB-C$_{10}$**, **TB-Si$_{4-3}$**, **TB-Si$_{3-3}$** and PTAA as HTMs.